Supplemental Material to

53BP1 as a Potential Predictor of Response in PARP Inhibitor-Treated Homologous Recombination-Deficient Ovarian Cancer

Rachel M. Hurley, Andrea E. Wahner Hendrickson, Daniel W. Visscher, Peter Ansell, Maria I. Harrell, Jill M. Wagner, Vivian Negron, Krista M. Goergen, Matthew J. Maurer, Ann L. Oberg, X. Wei Meng, Karen S. Flatten, Maja J. A. De Jonge, Carla D. Van Herpen, Jourik A. Gietema, Rutger H.T. Koornstra, Agnes Jager, Martha W. den Hollander, Matthew Dudley, Stacey P. Shepherd, Elizabeth M. Swisher, Scott H. Kaufmann

Supplemental Table 1.

Genes Assessed for Mutations in BROCA Analysis

ATM	ERCC3	MLH1	RAD51D
ATR	ERCC4	MRE11A	RBBP8
BABAM1	ERCC5	MSH2	RECQL
BAP1	ERCC6	MSH6	RIF1
BARD1	EZH2	NBN	RINT1
BLM	FAM175A	NEIL1	SLX4
BRCA1	FANCA	PALB2	SMARCA4
BRCA2	FANCB	PARP1	TOPBP1
BRCC3	FANCC	PAXIP1	TP53
BRE	FANCE	PIK3CA	TP53BP1
BRIP1	FANCF	PMS2	UBE2T
CDH4	FANCG	POLD1	UIMC1
CDK12	FANCI	POLE	USP28
CHD4	FANCL	POLQ	WRN
CHEK1	FANCM	PPM1D	XPA
CHEK2	GEN1	PTEN	XPC
DCLRE1C	HELQ	RAD50	XRCC2
DDB1	ID4	RAD51	XRCC3
ERCC1	LIG4	RAD51B	XRCC4
ERCC2	MAD2L2	RAD51C	XRCC5
			XRCC6

Supplemental Table 2

Response to Most Recent Platinum Therapy Among Responders and Non-responders

Time to Progression	Responders	Non-Responders
< 6 months	3	21
6 – 12 months	3	3
> 12 months	0	0

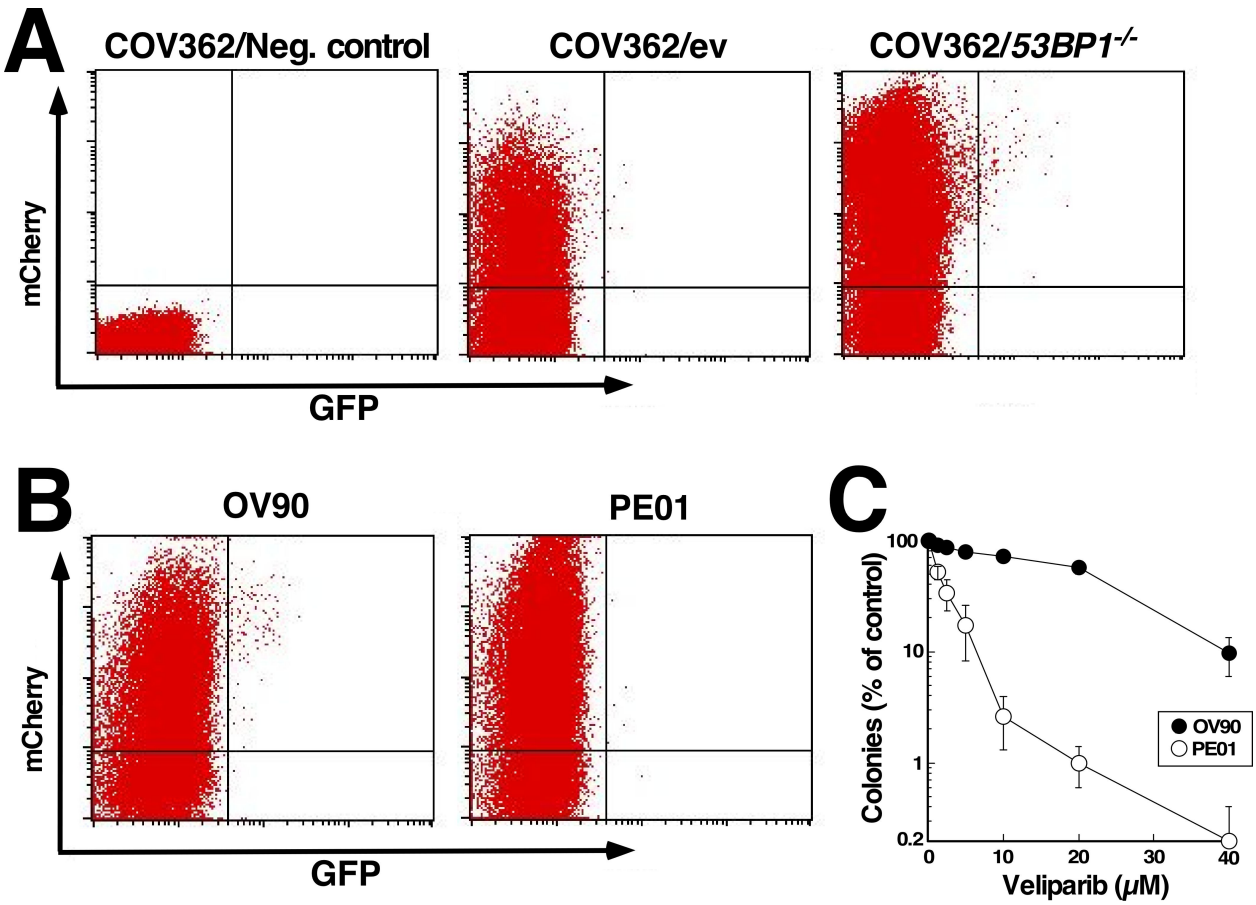

Supplemental Figure S1. Enhanced reactivation of DR-GFP in BRCA1-deficient COV362 ovarian cancer cells after *53BP1* gene disruption. A, A pool of COV362 cells transduced with pLK.01 puro without (upper middle panel) or with guide RNA targeting *53BP1* (upper right panel) were transfected with DR-GFP (as a substrate for the HR repair machinery) and empty vector (not shown) or plasmid encoding I-SceI and with pCherry (to mark successfully transfected cells with the mCherry protein). Forty-eight hours after transfection, cells were subjected to multiparameter flow cytometry as described in the Methods. Untransfected cells (upper left panel) were used to set gates. **B,** HR-proficient OV90 cells (left panel) and *BRCA2*-mutant PE01 cells (right panel) served as positive and negative controls, respectively for the HR assay depicted in panel A. Summarized results from multiple assays are shown in Fig. 1. **C,** cell lines used as controls in the HR assays were examined for ability to form colonies in the presence of the indicated veliparib concentrations. Error bars, ± SEM from 3 independent assays.

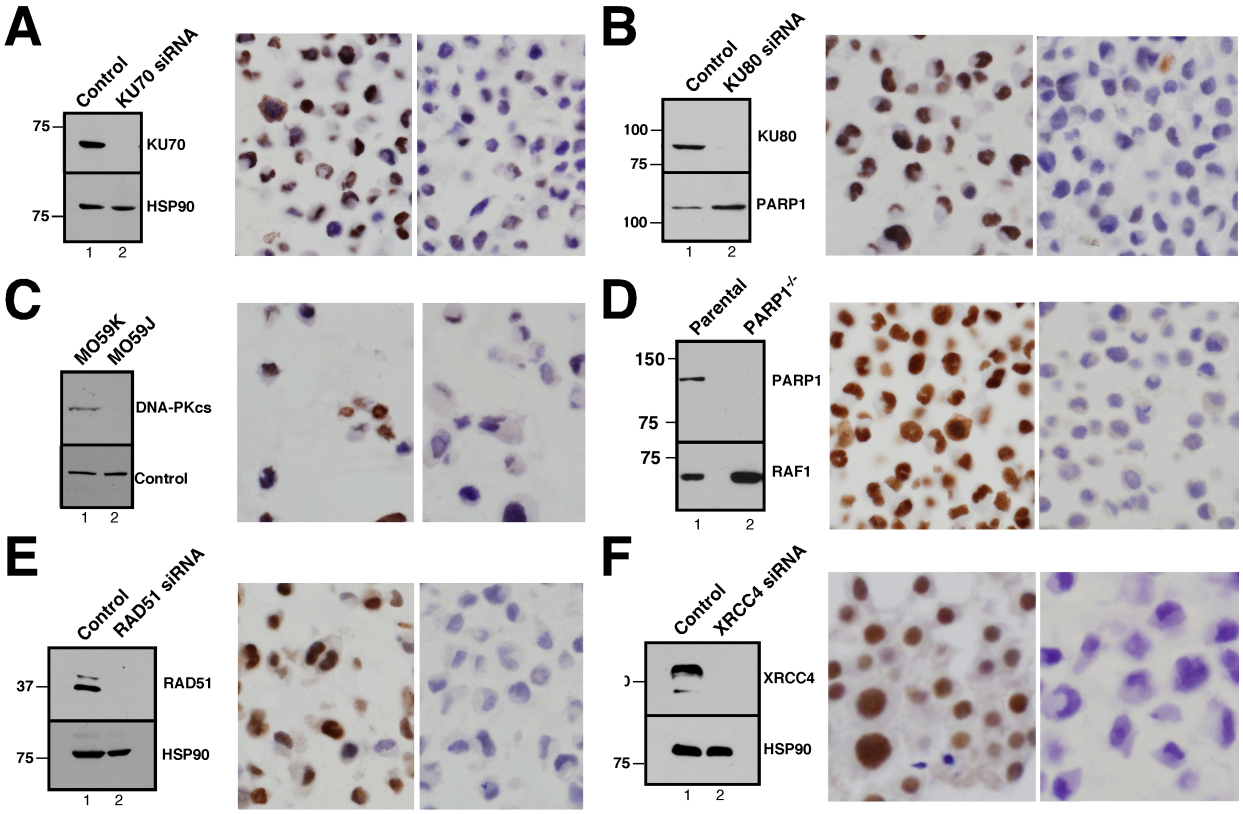

Supplemental Figure S2. IHC assay validation for KU80, DNA-PK$_{CS}$, KU70, XRCC4, RAD51, and PARP1. Ovcar8 cells transfected with the indicated siRNA (**A, B, E, and F**), parental MO59J cells lacking DNA-PK$_{CS}$ and a derivative transfected with the DNA-PK$_{CS}$ cDNA (**C**), or parental HCT116 cells and a clone with the *PARP1* gene interrupted (**D**) were subjected to SDS-PAGE and immunoblotting (left panels) or stained for the indicated antigen (right panels) to confirm antibody specificity. In additional experiments, we observed that over half of commercially available antibodies credentialed for detection of these antigens failed this specificity test (data not shown).

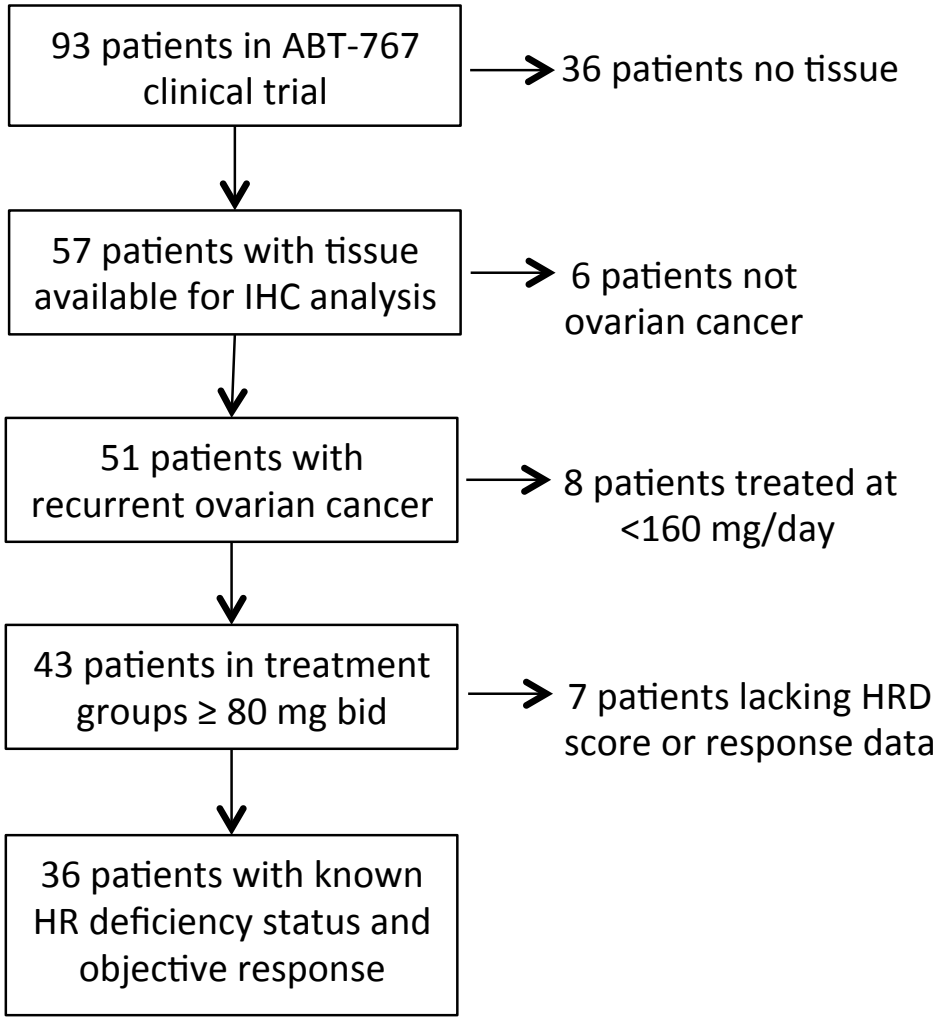

Supplemental Figure S3. Summary of clinical samples from ABT-767 clinical trial. In the present study, 36 samples from ovarian cancer patients treated with >160 mg/d ABT-767 who had archival diagnostic specimens, carcinoma HRD scores (Myriad) and response results were analyzed for DNA repair protein expression by IHC as described.

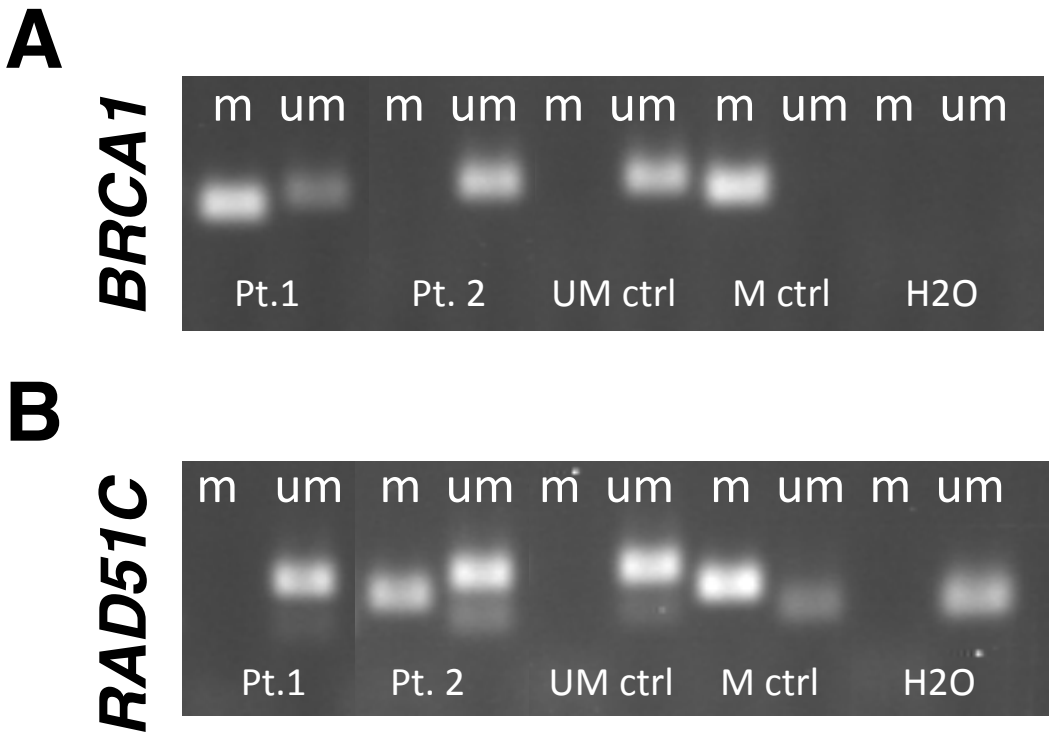

Supplemental Figure S4. Methylation analysis in HRD carcinomas without *BRCA1* or *BRCA2* mutations. In carcinomas that i) were deficient in HR as determined by the Myriad HRD assay but did not harbor a deleterious *BRCA1* or *BRCA2* mutation and ii) for which tissue was available for additional analysis, bisulfate sequencing was performed to visualize methylated (m) and unmethylated (um) DNA. The second round of bisulfate sequencing showed *BRCA1* promoter hypermethylation in Patient 1 (**A**) and *RAD51C* promoter hypermethylation in Patient 2 (**B**). Unmethylated controls (UM ctrl) and methylated controls (M ctrl) were utilized in both analyses. Nonadjacent lanes from a single photographic exposure have been juxtaposed to create each panel.

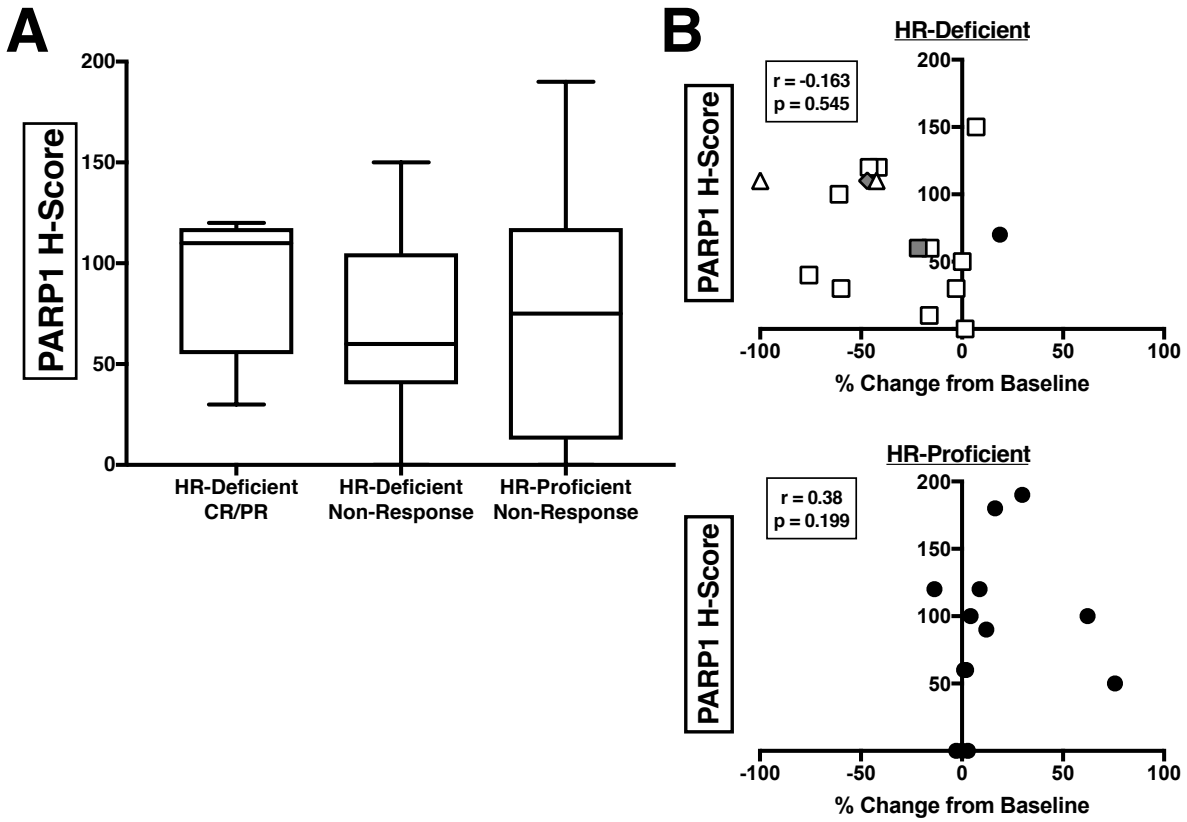

Supplemental Figure S5. PARP1 expression by IHC does not associate with response. Modified H-scores for PARP1 protein level did not differ between responders and non-responders by objective response (**A**) or percent change in tumor cross sectional area from baseline (**B**) in HR-deficient or HR-proficient ovarian cancers. HR gene alterations are denoted as mutations (white) or methylation (grey) of *BRCA1* (squares), *BRCA2* (triangle), or *RAD51C* (diamond).

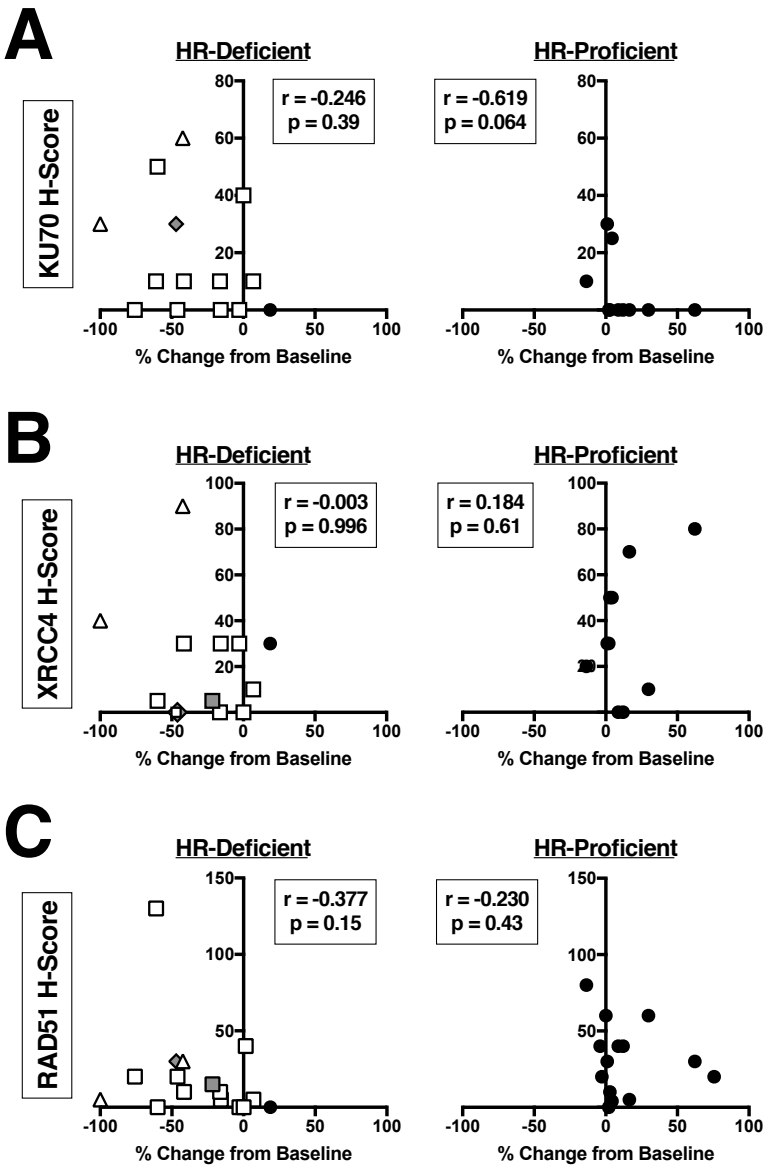

Supplemental Figure S6. Expression of KU70, XRCC4, or RAD51 does not correlate with change in tumor size. Modified H-score determined by evaluation of immunohistochemical staining was compared to percent change in tumor cross-sectional area from baseline [19] for KU70 (**A**), XRCC4 (**B**), and RAD51 (**C**). Carcinomas were segregated by HRD score, with HR-deficient shown on the left and HR-proficient shown on the right, and analyzed for Spearman correlation coefficients. HR gene alterations are denoted as mutations (white) or methylation (grey) of *BRCA1* (squares), *BRCA2* (triangle), or *RAD51C* (diamond).